

Theoretical analysis of neutron scattering results for quasi-two dimensional quantum anti-ferromagnet - possible role of Berezinskii - Kosterlitz - Thouless transition

Subhajit Sarkar,^{*} Ranjan Chaudhury,[†] and Samir K Paul[‡]
*S. N. Bose National Centre For Basic Sciences, Block - JD,
Sector - III, Salt Lake, Calcutta - 700 098, India*

(Dated: December 7, 2024)

Abstract

The available results from the inelastic neutron scattering experiment performed on the quasi-two dimensional spin- $\frac{1}{2}$ anti-ferromagnetic material La_2CuO_4 have been analysed theoretically. The formalism of ours is based on a semi- classical like treatment involving a model of an ideal gas of mobile vortices and anti-vortices built on the background of the Néel state, using the bipartite classical spin configuration corresponding to an XY- anisotropic Heisenberg anti-ferromagnet on a square lattice. The results for the integrated intensities for our spin- $\frac{1}{2}$ model corresponding to different temperatures, show occurrence of vigorous unphysical oscillations, when convoluted with a realistic spectral window function. Use of a refined realistic spectral window function however, minimizes unwanted oscillations but, the negative values of integrated intensity still persist within the experimental range. These results indicate failure of the semi-classical theoretical model of ideal vortex/anti-vortex gas. A full quantum formalism and treatment seem essential for treating such low spin systems. Furthermore, a severe disagreement is found to occur between the integrated intensities at finite values of energy transfer obtained theoretically from the present formalism and those obtained experimentally. This further suggests strongly that the full quantum treatment should also incorporate the interaction between the fragile-magnons and the vortices/merons (and anti-vortices/anti-merons).

^{*} subhajit@bose.res.in

[†] ranjan@bose.res.in

[‡] smr@bose.res.in

I. INTRODUCTION

Spin dynamics in low dimensional magnetic systems have received a significant research interest in the past three decades [1–31]. Different types of one and quasi-one dimensional as well as two and quasi-two dimensional systems have been studied both experimentally and theoretically to probe and understand the spin dynamics arising from the conventional spin wave excitations and their interactions, as well as from vortex/meron and soliton like topological excitations [15–17, 19, 20, 27]. In many of these systems the topological excitations of soliton and vortex/meron type occur naturally as they are thermodynamically feasible.

Motivated by the distinct possibilities of applications towards building of magnetic devices, the quasi-two dimensional systems have attracted a renewed research interest in recent times. Magnetic vortices present in these systems, have proved to be potential candidates for switching devices [32–35]. Direct experimental evidences of such vortices have been verified by both the Magnetic Force Microscopy (MFM) and the spin-polarized Scanning Tunnelling Microscopy (STM) [36, 37].

The spin dynamics in many of the above magnetic systems has been investigated experimentally using the Inelastic Neutron Scattering (INS) and the Nuclear Magnetic Resonance (NMR) techniques. These include quasi-one dimensional systems such as $CsNiF_3$, layered systems such as K_2CuF_4 , Rb_2CrCl_4 , $LiCrO_2$, magnetically intercalated graphites, layered ruthenates, layered manganites and the high- T_C cuprates [16–18, 20–29, 31]. In the INS experiments, performed on the several of the above materials, the existence of a “central peak” (at $\hbar\omega = 0$) has been observed in the plot for the dynamical structure function $S(\mathbf{q}, \omega)$ vs. neutron energy transfer ‘ $\hbar\omega$ ’ in the constant ‘ \mathbf{q} ’ scan [21, 22]. This finding further serves as the motivation behind the huge variety of experiments performed on the layered magnetic systems. Moreover, the advancement of numerical and computational techniques also contributed to the understanding of the possible role of both the spin wave and topological excitations in emergence of the central peak.

Kosterlitz and Thouless, and Berezinskii independently introduced the concept of vortex and anti-vortex like topological spin excitations in the two dimensional classical magnetic (spin) systems [38–40]. According to their ideas, there exists a non-conventional topological phase transition (known as Berezinskii- Kosterlitz- Thouless or BKT transition) characterized by the crossover between binding to unbinding phases of vortex- anti-vortex pairs at a

transition temperature T_{BKT} . Below this temperature all the vortices and anti-vortices are in a bound state and above this temperature some of them start moving freely. Further analytical and numerical studies and suitable extension of these approaches led to the proposal for the existence of topological vortices and anti-vortices in both ferromagnetic and anti-ferromagnetic XY model and merons and anti-merons in XY- anisotropic Heisenberg model on two- dimensional lattices [41–46]. Approximate analytical and Monte Carlo-Molecular Dynamics (MCMD) simulations have suggested that the freely moving topological excitations in the regime $T > T_{BKT}$ contribute non-trivially to the spin-spin correlation and give rise to the “central peak”, as mentioned above [41–44]. The occurrence of such a “central peak” in quasi-two dimensional magnetic systems is now unanimously believed to be the signature for the dynamics of mobile topological excitations.

In the context of two-dimensional magnetism, the undoped (anti-ferromagnetic and non-superconducting) phases of the high T_c cuprate systems are believed to be excellent examples of two dimensional XY anisotropic Heisenberg Hamiltonian in an appropriate temperature regime. One member of this class of systems is La_2CuO_4 , on which extensive INS experiments have been performed [30, 31]. This is a truly spin-1/2 layered anti-ferromagnet. The intra-layer integrated intensity corresponding to the results of INS experiment performed on La_2CuO_4 , exhibits a central peak when plotted against the neutron energy transfer $\hbar\omega$ (or frequency ‘ ω ’).

It has been shown that the results of vortex gas phenomenology and numerical simulations lead to an anomaly in the case of layered anti-ferromagnetic systems having very low spin values ($S=1/2$) [47]. Strikingly enough, the value of T_{BKT} obtained from Renormalization group analysis and numerical simulations is four (4) times the value of T_{BKT} calculated from the classical expression obtained by Kosterlitz and Thouless [47]. Furthermore, in our previous work we have already established that for quasi-two dimensional ferromagnetic systems having low spin values ($S= 1/2$) the semi-classical like treatment involving the ideal gas of unbound vortices/merons and anti-vortices/anti-merons corresponding to high temperature regime $T > T_{BKT}$ fails in explaining the experimental situation and exhibits unphysical behaviour [48]. In this case the theoretical dynamical structure function (DSF) turns out to be negative for a wide range of energy transfers! However the range, over which the theoretical DSF remains positive, increases when the value of the spin is increased [48]. These facts motivate us to investigate and test in detail the applicability of the semi-classical-like treat-

ment mentioned above to the INS results corresponding to real anti-ferromagnetic systems with $S=1/2$. For this exercise we select La_2CuO_4 as the reference system [30, 31].

The plan of the paper is as follows:- in section II we describe the formulation of our semi-classical like treatment; in section III we discuss our calculations and results and finally in section IV the conclusions and discussions of our present investigation are presented.

II. MATHEMATICAL FORMULATION

The dynamics of mobile vortices/merons and anti-vortices/anti-merons in an anti-ferromagnetic system on a two-dimensional square lattice have been analysed both analytically and numerically [41–45]. The analytical studies have been performed by assuming a classical ideal gas of vortices/merons where the vortices/merons obey Maxwell’s velocity distribution. The model system is described the XY-anisotropic Heisenberg (XXZ) Hamiltonian, viz.,

$$\mathcal{H} = -J \sum_{\langle ij,pq \rangle} (S_{ij}^x S_{pq}^x + S_{ij}^y S_{pq}^y + \lambda S_{ij}^z S_{pq}^z), \quad (1)$$

where $\langle ij,pq \rangle$ label the nearest neighbour sites on a two-dimensional square lattice and $J(< 0)$ is the anti-ferromagnetic exchange coupling. Here λ is the anisotropy parameter whose XY and isotropic Heisenberg limit correspond to $\lambda = 0$ and 1, respectively.

The structures of the vortices/merons have been obtained by solving the classical equations of motion corresponding to the Hamiltonian given by eqn. (1). In deriving the classical equations of motion the spins have been considered to be classical object (classical spin fields $S(\mathbf{r}, t)$) as a function of position coordinates and time, which are defined on the entire lattice. At even or odd lattice sites these spin fields become identical to the following bi-partite spin configurations:

$$\begin{aligned} S_{ij}^{even} &= +S[\sin(\Theta_{ij} + \theta_{ij}) \cos(\Phi_{ij} + \phi_{ij}), \sin(\Theta_{ij} + \theta_{ij}) \sin(\Phi_{ij} + \phi_{ij}), \cos(\Theta_{ij} + \theta_{ij})], \\ S_{ij}^{odd} &= -S[\sin(\Theta_{ij} - \theta_{ij}) \cos(\Phi_{ij} - \phi_{ij}), \sin(\Theta_{ij} - \theta_{ij}) \sin(\Phi_{ij} - \phi_{ij}), \cos(\Theta_{ij} - \theta_{ij})], \end{aligned} \quad (2)$$

where ‘*even*’ and ‘*odd*’ signifies the two different sub-lattices [49]. The static spin configuration corresponding to the merons are described by the capital angles $\Theta(\mathbf{r})$ (polar) and $\Phi(\mathbf{r})$ (azimuthal), and the time dependant small angles $\theta(\mathbf{r}, t)$ and $\phi(\mathbf{r}, t)$ describes the corresponding deviations from the static structure due to the motion of the merons and the

spin dynamics above BKT transition temperature [44, 45]. The expression of the vortex core radius is given by [44, 45]

$$r_v = \frac{a}{2} \sqrt{\frac{\lambda}{1-\lambda}}. \quad (3)$$

From the above considerations the in-plane dynamical structure function (in-plane DSF) $S^{xx}(\mathbf{q}, \omega)$ is given by,

$$S^{xx}(\mathbf{q}, \omega) = \frac{1}{8\pi} \frac{\gamma^3 \xi^2}{(\omega^2 + \gamma^2 [1 + (\xi \mathbf{q}^*)^2])^2}, \quad (4)$$

for $S = \frac{1}{2}$, with $\gamma = \frac{\sqrt{\pi} \bar{u}}{2\xi}$, where $\mathbf{q}^* = (\mathbf{q}_0 - \mathbf{q})$; $\mathbf{q}_0 = (\pi/a, \pi/a)$. The above expression for the in-plane dynamical structure function is a squared Lorentzian exhibiting a central peak at $\omega = 0$ in ' ω '-space for constant \mathbf{q} -scan and exhibiting a central peak at the zone boundary of the first Brillouin Zone (BZ) in the ' q ' space for constant ω -scan [44, 45]. In the above expression \bar{u} is the root mean square (rms) velocity of the vortices and is given by,

$$\bar{u} = \sqrt{b\pi} \frac{JS(S+1)a^2}{\hbar} (\sqrt{n_v^f}) \tau^{-1/4}, \quad (5)$$

where $n_v^f \sim \xi^{-2}$ is the density of free vortices at $T > T_{BKT}$ [41]. Here $\xi = \xi_0 e^{b/\sqrt{\tau}}$ is the intra-layer two-spin correlation length due to the presence of vortices, where ξ_0 is of the order of lattice spacing ' a '; $\tau = (\frac{T}{T_{BKT}} - 1)$ is the reduced temperature and b is a dimensionless parameter [22, 47] whose numerical value is generally around 1.5. The quantity $S^{xx}(\mathbf{q}, \omega)$ is sensitive to the in-plane structure of the vortices/merons [44, 45].

Again the effective analytical expression for the out-of-plane dynamical structure function (out-of-plane DSF) $S^{zz}(\mathbf{q}, \omega)$ in the limit of very small ' q ' is given by [44, 45],

$$S^{zz}(\mathbf{q}, \omega) = \frac{n_v^f \bar{u}}{32(1+\lambda)^2 J^2 \sqrt{\pi} q^3} \exp[-(\frac{\omega}{\bar{u}q})^2]. \quad (6)$$

The above form of the out-of-plane dynamical structure function is a Gaussian, exhibiting again a central peak at $\omega = 0$, when plotted in the constant \mathbf{q} -scan. The function $S^{zz}(\mathbf{q}, \omega)$ is sensitive to the out-of-plane shape of the vortices/merons [44, 45].

In the case of layered systems, in a suitable regime in the parameter space comprising of temperature and wave vector where these systems behave effectively as two-dimensional systems, the integrated intensity corresponding to a typical inelastic neutron scattering experiment is given by [15, 50, 51],

$$I(\omega) = \int \sum_{\alpha} S^{\alpha\alpha}(\mathbf{q}_{2D}, \omega) dq_x dq_y, \quad (7)$$

where the quantity $S^{\alpha\alpha}(\mathbf{q}_{2\mathbf{D}}, \omega)$ represents the intra-layer in-plane spin dynamical structure function when $\alpha = x$ and y and the intra-layer out-of-plane spin dynamical structure function when $\alpha = z$.

The approach in our present work is quite similar to that adopted earlier in the case of ferromagnetic systems [48]. In order to compare theory with experiment the dynamical structure function, obtained from the model under consideration, is multiplied with the resolution function $R(t)$ (in time domain) or convoluted with $\tilde{R}(\omega - \omega')$ (in the frequency domain), as has been done in the case of ferromagnetic system [48, 50, 52]. Hence, the components of the convoluted integrated intensity comes out to be,

$$I_{conv}^{\alpha\alpha}(\omega) = \int dq_x dq_y \int d\omega' \tilde{R}(\omega - \omega') S^{\alpha\alpha}(\mathbf{q}_{2\mathbf{D}}, \omega'). \quad (8)$$

The resolution function has to be chosen in such a way that minimum ripples occur at the end points of the resolution width. The different parameters of the resolution function can be obtained from the resolution half width or the full width at the half maximum (FWHM) which are quoted in the experiments. Since X and Y components of the spins are symmetric i.e., $S^{xx}(\mathbf{q}, \omega) = S^{yy}(\mathbf{q}, \omega)$ the total intensity comes out to be,

$$I(\omega) = 2I^{xx}(\omega) + I^{zz}(\omega). \quad (9)$$

Furthermore, keeping in mind the low spin situation the quantum mechanical detailed balance condition is incorporated in our formalism [53]. Then semi-classical estimate for $I(\omega)$, denoted by $I_{SC}(\omega)$ is recovered by the relation,

$$I_{SC}(\omega) = \frac{2}{1 + \exp(\frac{-\hbar\omega}{k_B T})} I(\omega), \quad (10)$$

where the factor $\frac{2}{1 + \exp(\frac{-\hbar\omega}{k_B T})}$ is the detailed balance factor and is called the Windsor factor [54, 55]. The subscript ‘SC’ stands for the term semi-classical.

As has been pointed out in the case of ferromagnetic systems, this approach of ours is truly ‘semi-classical-like’ in the sense that the expression for the rms vortex velocity ‘ \bar{u} ’, as given in eqn. (4), contains ‘ \hbar ’ and in addition the quantum mechanical detailed balance condition has been incorporated through the Windsor factor[48].

III. CALCULATIONS AND RESULTS

In this work the formalism of Section II is applied to an anti-ferromagnetic material La_2CuO_4 on which inelastic neutron scattering experiments (INS) involving polarized neutron beam have been performed [30, 31]. The material is an XY-anisotropic quasi-two-dimensional spin 1/2 quantum Heisenberg anti-ferromagnet. The magnetic lattice structure of it is composed of stacking of two-dimensional square lattices [30, 31]. The spin Hamiltonian relevant to the above material is given by,

$$\mathcal{H} = \underbrace{\left(-J \sum_{\langle i,j \rangle} \mathbf{S}_i \cdot \mathbf{S}_j + J_A \sum_{\langle i,j \rangle} S_i^z S_j^z\right)}_{\text{intra-layer part}} - \underbrace{J' \sum_{\langle i,k \rangle} \mathbf{S}_i \cdot \mathbf{S}_k}_{\text{inter-layer part}} \quad (11)$$

where $\langle i, j \rangle$ represents the intra-layer nearest neighbour interaction and $\langle i, k \rangle$ represents the inter-layer nearest neighbour interaction. In the above Hamiltonian, J is the isotropic part of the intra-layer exchange coupling, J_A is anisotropic part of the intra-layer exchange coupling and J' is the inter-layer exchange coupling. The ordering temperature i.e., the Néel temperature for the quasi-two dimensional system (La_2CuO_4) is given by $T_N = 240$ K. The intra-layer part of the above Hamiltonian (11) can be simplified, by expressing $(J - J_A)$ as λJ , to obtain the model Hamiltonian (1), where λ is the anisotropy parameter. The relevant physical parameters corresponding to La_2CuO_4 are given in the TABLE I [57].

Parameter	Magnitude
J (intra-layer)	~ 1345 K
J_A (intra-layer)	~ 0.269 K
J' (inter-layer)	~ 0.04 K
anisotropy parameter (λ)	0.9998
lattice parameter(a)	5.39 Å

TABLE I. Relevant parameters for La_2CuO_4

Next we try to determine the temperature range over which the material La_2CuO_4 behaves effectively as a two-dimensional material. From the neutron scattering data for quasi-two-dimensional spin 1/2 XY-anisotropic ferromagnet K_2CuF_4 , it was found that in a

temperature regime $T_1 \leq T \leq T_2$, where the lower (T_1) and the upper (T_2) limits are defined by the following relations,

$$\begin{aligned}\xi(T_1) &= \sqrt{\frac{|J|}{|J'|}} \\ \xi(T_2) &= \sqrt{\frac{|J|}{|J_A|}}\end{aligned}\quad (12)$$

the system behaves as a 2D XY-like anisotropic system [21, 22]. Assuming that the above phenomenological argument holds for the layered anti-ferromagnetic systems as well, we

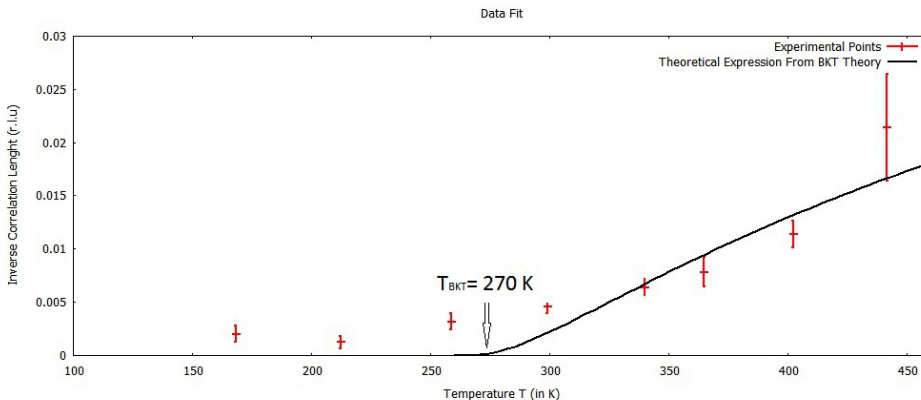


FIG. 1. *Fitting of the experimentally obtained inverse correlation length with the corresponding theoretical expression (see eqn. (13)). Solid line corresponds to the theoretical expression. BKT transition temperature is $T_{BKT} = 270K$.*

determine the above two temperature limits as $T_1 \approx 260K$ and $T_2 \approx 360K$ for La_2CuO_4 . Within this temperature regime the Hamiltonian (11) can effectively be represented by the Hamiltonian (1). It is worthwhile to point out that since in the above temperature regime the system is effectively a two-dimensional one, long range anti-ferromagnetic ordering is absent in this regime [58]. Further, within the above mentioned temperature range the BKT inspired ideal vortex/meron- gas phenomenology is valid and we can therefore use the theoretical expression for the inverse correlation length (expressed in r.l.u),

$$\kappa(T) = \frac{1}{\pi} e^{-b/\sqrt{\tau}} \quad (13)$$

as predicted by Kosterlitz and Thouless, to fit the experimentally obtained inverse correlation length [38]. This gives the value of the BKT transition temperature as $T_{BKT} \approx 270K$ for

La_2CuO_4 (see FIG. 1). In this work we shall make use of the above value of T_{BKT} to calculate the convoluted in-plane integrated intensity, $I_{conv}^{xx}(\omega)$ and the convoluted out-of-plane integrated intensity $I_{conv}^{zz}(\omega)$, by making use of eqns. (4) to (6), and then eqns. (7) and (8).

We now study the convoluted in-plane integrated intensities $I_{conv}^{xx}(\omega)$ at different temperatures. The expression for the $I_{conv}^{xx}(\omega)$ is given by eqn. (8) with $\alpha = x$, where the in-plane DSF, $S^{xx}(\mathbf{q}_{2D}, \omega)$ is given by eqn. (4). In the experimental investigations on La_2CuO_4 , to find the neutron intensity as a function of momentum transfer ' $\hbar\mathbf{q}$ ' the scans in the ' \mathbf{q} '-space have been performed about the zone boundary of the first BZ within the range, $-0.1 \leq \mathbf{q}^* \leq 0.1$, expressed in r.l.u [30, 31]. In calculating $I_{conv}^{xx}(\omega)$ using eqn. (13) we have also made use of the above mentioned regime only. The resolution function has been chosen in the form of the Tukey window to convolute the in-plane DSF. This is one of the most commonly used spectral smoothing functions in the field of spectral analysis [59, 60]. The experimental resolution width is 1.4 meV at the full width at half maximum (FWHM) as specified in the experiment [30, 31]. We compute $I_{conv}^{xx}(\omega)$ for four different temperatures, viz., 290 K, 320 K, 350 K and 375 K. The semi-classical convoluted in-plane integrated in-

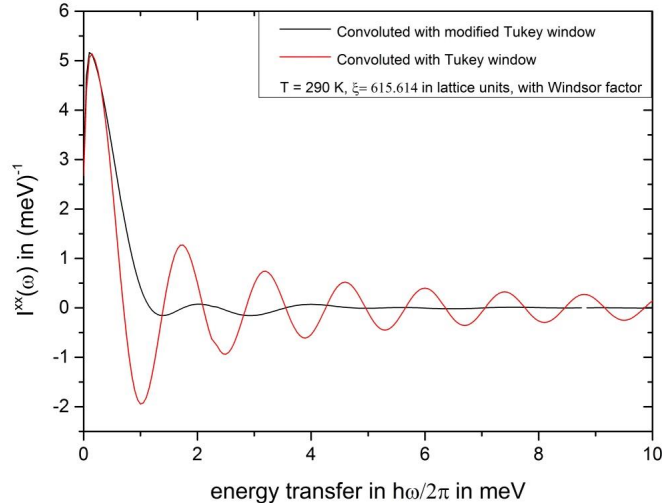


FIG. 2. The plot of convoluted in-plane integrated intensity $I_{conv}^{xx}(\omega)|_{SC}$ at 290 K. The red solid line corresponds to the $I_{conv}^{xx}(\omega)|_{SC}$ obtained by using the Tukey window function (see (A2)). The black solid line corresponds to the $I_{conv}^{xx}(\omega)|_{SC}$ obtained by using the modified Tukey window function (see (A5)). The rms velocity at this temperature is $\bar{u} = 0.00365 \frac{a}{t_{nat}}$

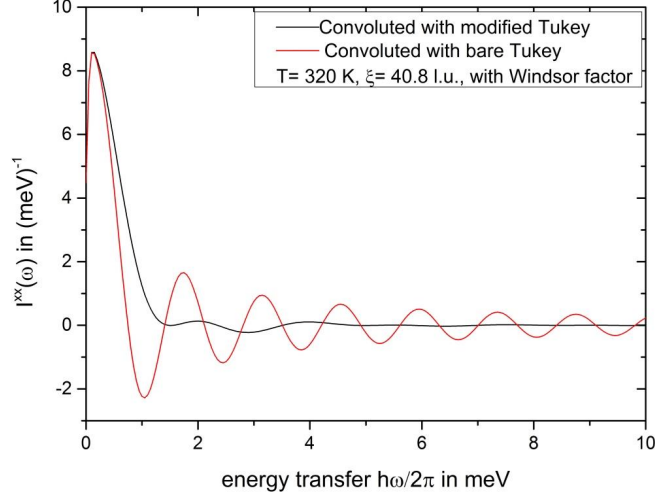


FIG. 3. The plot of convoluted in-plane integrated intensity $I_{conv}^{xx}(\omega)|_{SC}$ at 320 K. The red solid line corresponds to the $I_{conv}^{xx}(\omega)|_{SC}$ obtained by using the Tukey window function (see (A2)). The black solid line corresponds to the $I_{conv}^{xx}(\omega)|_{SC}$ obtained by using the modified Tukey window function (see (A5)). The rms velocity at this temperature is $\bar{u} = 0.0836 \frac{a}{t_{nat}}$

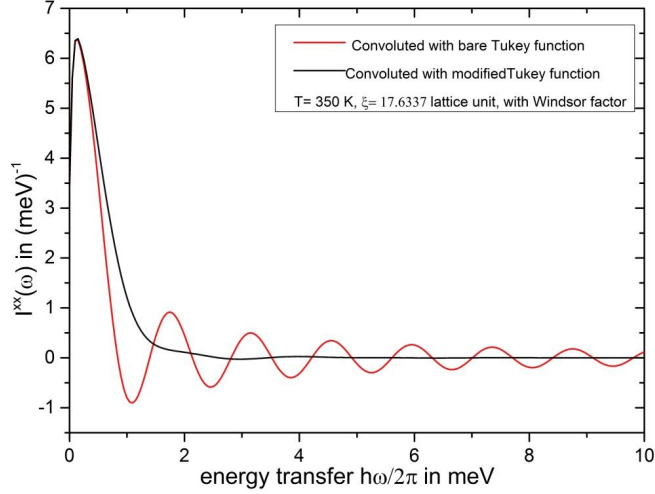


FIG. 4. The plot of convoluted in-plane integrated intensity $I_{conv}^{xx}(\omega)|_{SC}$ at 350 K. The black solid line corresponds to the $I_{conv}^{xx}(\omega)|_{SC}$ obtained by using the Tukey window function (see (A2)). The red solid line corresponds to the $I_{conv}^{xx}(\omega)|_{SC}$ obtained by using the modified Tukey window function (see (A5)). The rms velocity at this temperature is $\bar{u} = 0.085 \frac{a}{t_{nat}}$

tensities denoted by, $I_{conv}^{xx}(\omega)|_{SC}$ are plotted as functions of energy transfers in the FIGs. (2)

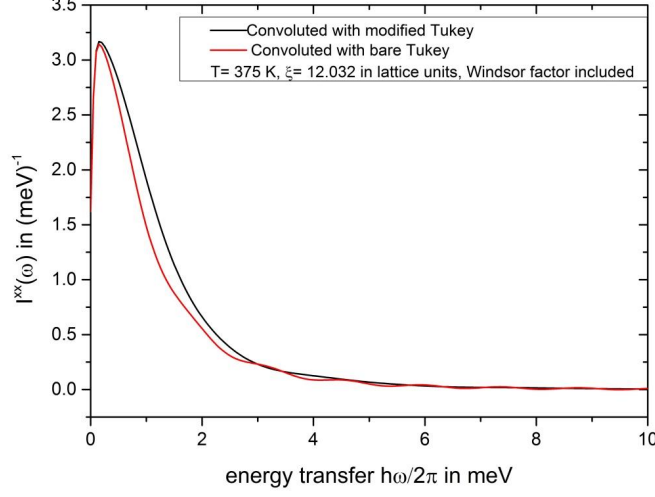


FIG. 5. The plot of convoluted in-plane integrated intensity $I_{conv}^{xx}(\omega)|_{SC}$ at 375 K. The red solid line corresponds to the $I_{conv}^{xx}(\omega)|_{SC}$ obtained by using the Tukey window function (see (A2)). The black solid line corresponds to the $I_{conv}^{xx}(\omega)|_{SC}$ obtained by using the modified Tukey window function (see (A5)). The rms velocity at this temperature is $\bar{u} = 0.2323 \frac{a}{t_{nat}}$

- (5), where eqns. (9) and (10) have been used. The figures clearly exhibit that $I_{conv}^{xx}(\omega)|_{SC}$ oscillates vigorously after convoluting with the Tukey function! This is quite contrary to what we experienced in the case of ferromagnet [48].

To avoid such unwanted oscillations we later tried performing the above calculations using a modified version of the Tukey function (see eqns. (A4) and (A5) in the Appendix). The integrated intensities corresponding to this new window function are also plotted in the same figures mentioned above. From these figures it is clearly visible that the unwanted oscillations diminish considerably when we use the modified Tukey function. Interestingly we notice that at higher temperatures around $1.29T_{BKT}$, i.e., at 350 K the oscillations have totally vanished with the use of new window function; however, magnitude of the theoretical $I_{conv}^{xx}(\omega)|_{SC}$, computed using the modified Tukey function, turns out to be negative, although the ‘central peak’ still persists. We further notice a slight shift in the position of the central peak. This is due to the inclusion of detailed balance condition. The important point here is that the shift is well within the resolution width 1.4 meV at the FWHM, and hence the peak is truly a central peak situated at $\hbar\omega = 0$.

More interestingly, the FIG. (5) indicates that at even higher temperature, viz., at around 375 K ($\approx 1.38T_{BKT}$) both the Tukey function and the modified Tukey function lead to very similar results. The unwanted oscillations are totally absent in the theoretical plot of $I_{conv}^{xx}(\omega)|_{SC}$ vs. energy transfers corresponding to both the resolution functions. It is worthwhile to mention that the corresponding temperature $T=375$ K ($> T_2$) falls just outside the range $T_1 \leq T \leq T_2$ within which the BKT phenomenology remains valid.

Exactly the same results hold for $I_{conv}^{yy}(\omega)|_{SC}$ which is obvious from the symmetry argument. The normalization factor required for the quantitative comparison between the theoretical and the experimental results is estimated from the neutron count corresponding to the experimental results for La_2CuO_4 .

We now evaluate the out-of-plane integrated intensity $I_{conv}^{zz}(\omega)|_{SC}$ for the same set of temperatures as have been considered earlier for the evaluation of $I_{conv}^{xx}(\omega)|_{SC}$. The expression for the $I_{conv}^{xx}(\omega)$ is given by, eqn. (8) with $\alpha = z$, where the out-of-plane DSF, $S^{zz}(\mathbf{q}_{2D}, \omega)$ is given by eqn. (6). In this case we find that the out-of-plane integrated

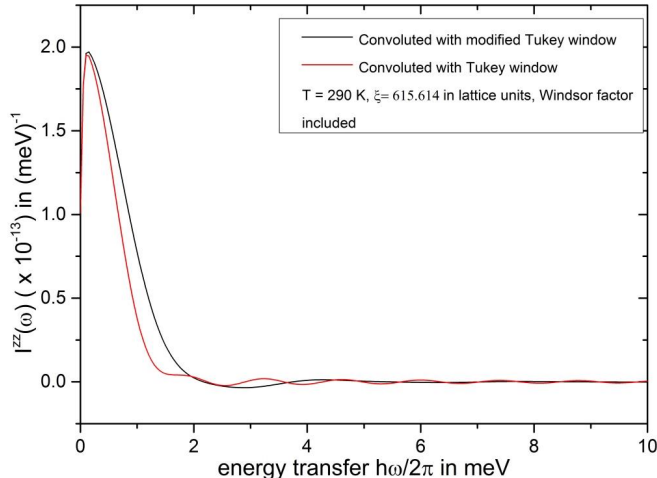


FIG. 6. The plot of convoluted out-of-plane integrated intensity $I_{conv}^{zz}(\omega)|_{SC}$ at 290 K. The red solid line corresponds to the $I_{conv}^{zz}(\omega)|_{SC}$ obtained by using the Tukey window function (see (A2)). The black solid line corresponds to the $I_{conv}^{zz}(\omega)|_{SC}$ obtained by using the modified Tukey window function (see (A5)). The rms velocity at this temperature is $\bar{u} = 0.00365 \frac{a}{t_{nat}}$

intensity oscillates only at lower temperatures near $T = T_{BKT}$ when the Tukey function is used for convolution. The use of modified Tukey function (see eqns. (A4) and (A5) in

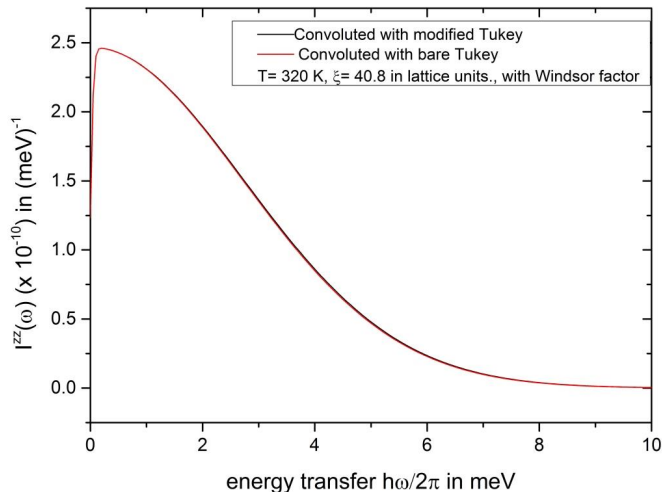


FIG. 7. The plot of convoluted out-of-plane integrated intensity $I_{conv}^{zz}(\omega)|_{SC}$ at 320 K. The red solid line corresponds to the $I_{conv}^{zz}(\omega)|_{SC}$ obtained by using the Tukey window function (see (A2)). The black solid line corresponds to the $I_{conv}^{zz}(\omega)|_{SC}$ obtained by using the modified Tukey window function (see (A5)). The rms velocity at this temperature is $\bar{u} = 0.0836 \frac{a}{t_{nat}}$

the Appendix) again suppresses the unwanted oscillations (see FIG. (6)) as before. At the higher temperatures away from T_{BKT} , the unwanted oscillations just vanish altogether and both the window functions produce the same results (see FIGs. (7) - (9)). It is worth recalling here that the magnitude of the out-of-plane integrated intensity is proportional to the density n_v^f and the rms velocity \bar{u} of the free vortices/merons. Since both density n_v^f and the rms velocity \bar{u} increases with increasing temperature the out-of-plane part of the spin-spin correlation (see eqns. (6) and (8)) acquire dominance (considerable magnitude) only at higher temperatures much above T_{BKT} .

Furthermore, the absolute magnitude of the integrated intensity $I_{conv}^{xx}(\omega)|_{SC}$ is higher (almost 10^7 times for the highest temperature considered here) than that of $I_{conv}^{zz}(\omega)|_{SC}$ at temperatures above T_{BKT} . This is so because, $I_{conv}^{zz}(\omega)|_{SC}$ is proportional to n_v^f and it increases with the increasing value of the rms velocity \bar{u} , and the typical energy scales involved in the dynamics of mobile vortices/merons corresponding to the anti-ferromagnetic system La_2CuO_4 are such that both n_v^f and \bar{u} are very small (compared to the case of ferromagnet where the free vortex number density turns out to be appreciable [48]). For the present case of La_2CuO_4 at $T = 350K$, the numerical value for the density of free vortices

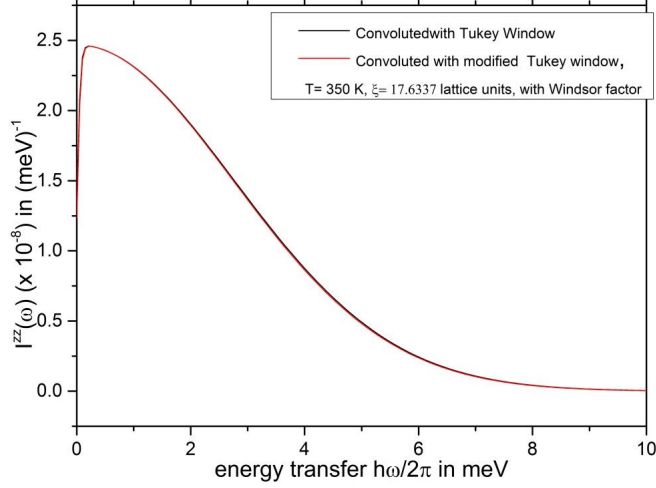


FIG. 8. The plot of convoluted out-of-plane integrated intensity $I_{conv}^{zz}(\omega)|_{SC}$ at 350 K. The red solid line corresponds to the $I_{conv}^{zz}(\omega)|_{SC}$ obtained by using the Tukey window function (see (A2)). The black solid line corresponds to the $I_{conv}^{zz}(\omega)|_{SC}$ obtained by using the modified Tukey window function (see (A5)). The rms velocity at this temperature is $\bar{u} = 0.085 \frac{a}{t_{nat}}$

comes out to be $n_v^f = 1.36 \times 10^{-4} a^{-2}$ and the same for the rms velocity comes out to be $\bar{u} = 9163 m/sec = 0.085 \frac{a}{t_{nat}}$, where $t_{nat} = \frac{2\hbar}{\sqrt{3}J}$ ($\approx 5 \times 10^{-15}$ sec) is the natural time scale for the system. In contrast, in the case of ferromagnetic system K_2CuF_4 the value of the density of free vortices was found to be $n_v^f = 1.009 \times 10^{-3} a^{-2}$ and that for the rms velocity was found to be $\bar{u} = 87.07 m/sec = 0.1352 \frac{a}{t_{nat}}$ at $T = 6.75K$, where $t_{nat} = 6.4 \times 10^{-13}$ sec is the natural time scale [48].

Interestingly enough, the unbound merons/vortices above T_{BKT} move much faster (with a rms velocity of 9163 m/sec at 350 K) than a typical Copper (Cu) atom whose rms velocity (generally considered to be the thermal velocity) is around 370.6 m/sec at 350 K.

The integrated intensities computed above correspond to the contributions only from the mobile vortices/merons. The experimental data whereas, contain contributions from both the mobile vortices/merons and fragile “spin wave like” modes. This spin wave like modes are damped and largely decaying above the Néel temperature. The extraction of the mobile vortex contribution from the experimental data is crucial for a more accurate comparison between the theoretical results and the experimental data and to do this one has to subtract the contributions from the above mentioned fragile “spin wave like” modes from

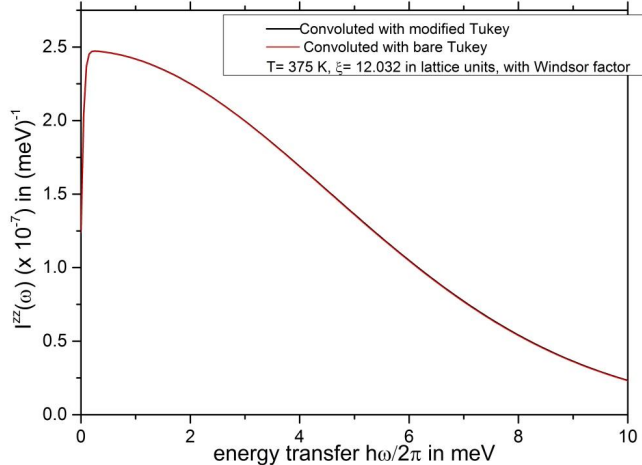


FIG. 9. The plot of convoluted out-of-plane integrated intensity $I_{conv}^{zz}(\omega)|_{SC}$ at 375 K. The red solid line corresponds to the $I_{conv}^{zz}(\omega)|_{SC}$ obtained by using the Tukey window function (see (A2)). The black solid line corresponds to the $I_{conv}^{zz}(\omega)|_{SC}$ obtained by using the modified Tukey window function (see (A5)). The rms velocity at this temperature is $\bar{u} = 0.2323 \frac{a}{t_{nat}}$

the experimental data. It is worth recalling that in the case of ferromagnetic system, the fragile mode contributions have been subtracted by assuming the fragile mode contributions above T_c to be the same as the usual spin wave contributions below T_c . This assumption is however valid if and only if the temperature under consideration is in the near vicinity of the Curie temperature (T_c) of the system [48].

In the present case corresponding to the anti-ferromagnetic system La_2CuO_4 , the situation is somewhat different from the case of ferromagnetic systems in the sense that the temperatures dealt with are far above the Néel temperature T_N . Hence the above mentioned procedure, which was followed for the ferromagnetic systems to subtract the fragile mode contributions, is not valid.

Moreover at any finite temperature above T_{BKT} , not all vortices/merons are freely moving and bound vortex-anti-vortex pair density remains finite. Hence, one has to estimate further the contribution from these bound vortex-anti-vortex pairs at different temperatures and subtract it from the experimental data. To estimate the bound vortex contribution we have tried to apply the same methodology that has been outlined and used earlier for the ferromagnetic system [48]. However, unlike the case of ferromagnet in this case the

methodology leads to an unphysical behaviour viz., the vanishing of the out-of-plane DSF (see eqn. (6)) in the limit $\bar{u} \rightarrow 0$. Hence the estimation of the bound vortex contribution has not been carried out here.

The above calculations for the components of integrated intensities enable us to estimate theoretically the total integrated intensity using (9). In FIGs. (10) and (11) the total

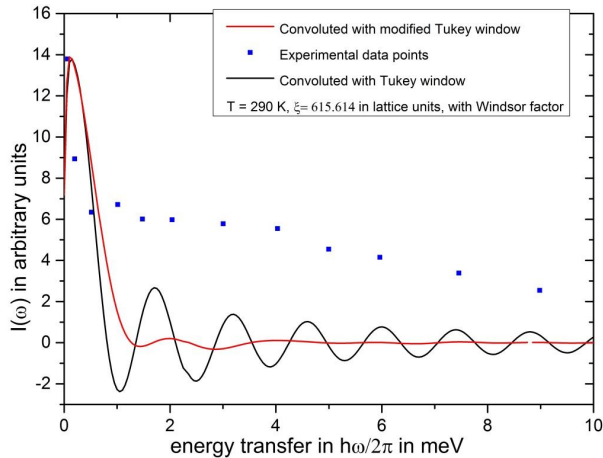


FIG. 10. The plot of convoluted total integrated intensity $I_{conv}(\omega)|_{SC}$ at 290 K. The red solid line corresponds to the $I_{conv}(\omega)|_{SC}$ obtained theoretically by using the Tukey window function (see (A2)). The black solid line corresponds to the $I_{conv}(\omega)|_{SC}$ obtained theoretically by using the modified Tukey window function (see (A5)). The dots are the experimental data. The rms velocity at this temperature is $\bar{u} = 0.00365 \frac{a}{t_{nat}}$

intensity $I_{conv}(\omega)|_{SC}$ has been compared to the experimental data at two different temperatures, viz., 290K and 350K respectively. The contributions from the fragile “spin-wave-like” modes can not be filtered out for the reasons stated earlier. It is clear from the FIG. (10) that the total intensity $I_{conv}(\omega)|_{SC}$ also oscillates vigorously at lower temperature around $T = 290K$ ($\approx 1.07T_{BKT}$), when convoluted with the Tukey function, due to the domination of in-plane correlations over the out-of-plane correlation. The oscillation is markedly minimized when the modified Tukey function (see eqns. (A4) and (A5)) is used. At this lower temperature the oscillations still persist even if we use the modified Tukey function. Besides, the theoretical results show negative values for $I_{conv}(\omega)|_{SC}$ with both the resolution function!

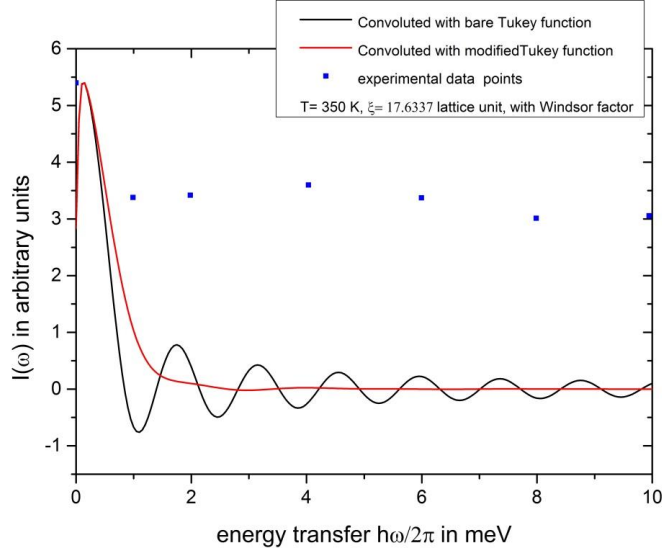


FIG. 11. The plot of convoluted total integrated intensity $I_{conv}(\omega)|_{SC}$ at 350 K. The red solid line corresponds to the $I_{conv}(\omega)|_{SC}$ obtained theoretically by using the Tukey window function (see eqn. (A2)). The black solid line corresponds to the $I_{conv}(\omega)|_{SC}$ obtained theoretically by using the modified Tukey window function (see eqn. (A5)). The dots are the experimental data. The rms velocity at this temperature is $\bar{u} = 0.085 \frac{a}{t_{nat}}$

On the other hand at higher temperatures, around 350 K ($\approx 1.29T_{BKT}$), a vigorous oscillation in $I_{conv}(\omega)|_{SC}$ is seen when the Tukey function is used, whereas the oscillations vanish when the modified Tukey function is used as window function (see FIG. (11)). Surprisingly, the values of $I_{conv}(\omega)|_{SC}$ come out to be negative, with both the resolution function, even at this higher temperature ($1.29T_{BKT}$). Moreover, the magnitude of the total intensity $I_{conv}(\omega)|_{SC}$, obtained theoretically at finite energy transfers, is very far from the corresponding values obtained in the experiment.

The inclusion of quantum mechanical detailed balance factor in our semi-classical like treatment has again caused a shift in the position of the central peak of the integrated total intensity at both the temperatures. However, this shift is well within the resolution width and therefore it is a genuine central peak at zero energy transfer.

To summarize, we find vigorous oscillation in the convoluted in-plane integrated intensity when the Tukey window is used. These oscillations vanish only at higher temperatures which are outside regime where the BKT phenomenology is valid. The use of a

modified/refined Tukey function substantially remove the unwanted oscillations in the convoluted in-plane integrated intensity $I_{conv}^{xx}(\omega)|_{SC}$. Strikingly enough, at $T = 350$ K ($1.29 T_{BKT}$), we still find negative values of $I_{conv}^{xx}(\omega)|_{SC}$ even using the modified Tukey window function. However, outside the temperature regime where the BKT phenomenology is valid, computations with both the window functions give very similar results for $I_{conv}^{xx}(\omega)|_{SC}$. The possible explanation for this is that at higher temperatures the quantum effects are less prominent even for $S = \frac{1}{2}$ anti-ferromagnet. Therefore, the modified Tukey window may actually be suppressing quantum fluctuation as well quite efficiently. The out-of-plane integrated intensities $I_{conv}^{zz}(\omega)|_{SC}$ (computed at different temperatures) are found to be sensitive to the choice of window function only at temperatures which are not very far from T_{BKT} (around $1.07 T_{BKT}$). Furthermore, it contributes negligibly to the total integrated intensity $I_{conv}(\omega)|_{SC}$ and hence the nature of the convoluted total integrated intensities at different temperatures turns out to be quite similar to that of the convoluted in-plane integrated intensities. However, the detailed quantitative comparison between the theoretical results and the experimental results corresponding to the total integrated intensities $I_{conv}(\omega)|_{SC}$ reveals that even though our “semi-classical like” theory is able to predict the occurrence of the central peak, the magnitudes of the $I_{conv}(\omega)|_{SC}$ for finite values of energy transfer, obtained from theoretical analysis, differ by a huge factor from the corresponding experimental values. This is unlike the situation with quasi-two dimensional $S = \frac{1}{2}$ ferromagnet K_2CuF_4 where we had obtained quite good quantitative agreement with experimental results [48].

It is worthwhile to mention that all the above results based on dilute vortex/meron gas phenomenology hold for unbound anti-vortices/anti-merons too.

IV. CONCLUSIONS AND DISCUSSIONS

It is a well known fundamental fact that the spin-dynamical structure function (DSF) and hence the integrated intensity corresponding to all real magnetic systems must be positive definite [15, 50, 51]. Our detailed calculations and analysis however, brings out an important fact that for quasi-two dimensional low-spin anti-ferromagnetic systems, the semi-classical treatment of ideal gas of mobile vortices/merons (anti-vortices/anti-merons) leads to negative values of total integrated intensities when convoluted with commonly used resolution functions. Similar results were obtained for $S = 1/2$ layered ferromagnets [48]. Such a be-

haviour is purely unphysical. Furthermore, we find vigorous oscillations in the theoretically obtained total integrated intensities which have been reduced substantially by modifying the window function used. However, the oscillations resulting from the convolution (with both the window function) vanish completely at $T = 375K$ ($1.38 T_{BKT}$) which falls just outside the regime of applicability of vortex/meron gas phenomenology. These facts point out to the inapplicability of the semi-classical vortex/meron gas phenomenology to the quasi-two dimensional low-spin anti-ferromagnetic systems and necessitates the demand for a full quantum treatment.

It is important to emphasize the fact that structure of the classical vortex/meron has been built in the background of the Néel state (see (2) of section II). Since the Néel state is not an exact ground state for the two-dimensional quantum anti-ferromagnetic spin systems, such a choice further adds to the reasons for the above mentioned unphysical behaviour.

We further find that the absolute magnitude of the out-of-plane integrated intensity is negligibly small compared to that of the in-plane integrated intensity for La_2CuO_4 . The former increases when the temperature is increased. This implies that the in-plane spin-spin correlation becomes dominant at lower temperature. It is expected that at fairly high temperatures (far away from T_{BKT} , around $1.38 T_{BKT}$ and above) the out-of-plane spin-spin correlation starts playing its role and thereby contribute appreciably to the total integrated intensity. Such a high temperature however, falls outside the regime ($260K \leq T \leq 360K$) where the BKT inspired phenomenology and our “semi-classical like” theory are applicable.

Keeping aside the occurrences of unphysical negative values of the integrated intensities obtained from our semi-classical-like theory the results agree with those from the experiment quite well, in terms of the existence of the central peak. Although the inclusion of the quantum mechanical detailed balanced condition shifts the position of the central peak, the peak still remains within the experimental resolution width justifying that the central peak is genuine one.

However, the quantitative comparison reveals that the magnitude of the integrated intensities for finite values of energy transfer, obtained from theory and experiment, disagree very strongly (see FIGs. (10) and (11)). This may originate from the interactions between the vortices/merons and the fragile spin-waves/ quantized fragile-magnon modes and subsequent formation of vortices/merons from such fragile magnons which is neglected in the theoretical model used here. Such a comparison for finite values of energy transfer become

even worse when the temperatures is increased. This is because, when the temperature rises the additional interactions processes mentioned above become more complicated and therefore is quite likely to contribute non-trivially to the DSF. At this point, it is worth mentioning that for ferromagnetic systems it has been shown that the formation of topological excitations of vortex/ meron from the fragile magnons and multi-magnon composites is quite plausible [61]. This process is expected to be operative in anti-ferromagnetic systems as well. Therefore, the interplay between the fragile magnons/multi-magnon composites and the vortices/merons is very crucial in the proper understanding of the dynamics of unbound vortices/merons (anti-vortices/anti-merons) in the quasi-two-dimensional low-spin anti-ferromagnetic systems. This further takes care of the fragile magnon contributions to the total integrated intensities as well which has not been filtered out from the experimental data (for the reasons stated earlier in the section III). In addition, the severe inadequacy of the semi-classical treatment in the case of quantum anti-ferromagnet may also contribute to this quantitative disagreement for the integrated intensities.

Our investigations presented in this communication brings out the fact that a complete quantum treatment is essential to describe the detailed features of the dynamics of mobile vortices/merons and anti-vortices/anti-merons corresponding the quasi-two-dimensional low-spin anti-ferromagnetic systems by taking into consideration the vortex/meron-fragile magnon interactions as well. Moreover, since the Néel state is not an exact ground state for the two-dimensional quantum spin systems the construction of the quantum vortices/merons in the complete quantum treatment has to be supplemented with proper choice of the ground state too. A theoretical framework had been developed earlier based on the spin coherent state path integral formalism to describe the topological properties of static vortices and anti-vortices [62–67]. An extension of this framework to the case mobile spin vortices/merons (and anti-vortices/anti-merons) is crucial for quantum mechanical calculations of the DSF and the integrated intensity as well. This would be taken up in future. This study of dynamics of the BKT vortices/merons may also provide very valuable contributions to the microscopic understanding of lightly doped anti-ferromagnetic cuprates [47, 68, 69]

Acknowledgements:

One of the authors (SS) acknowledges the financial support through Senior Research Fellowship (09/575 (0089)/2010 EMR-1) provided by Council of Scientific and Industrial Research (CSIR), Govt. of India.

Author contribution statement:

All authors have contributed equally to this communication.

Appendix A: The Tukey and the modified Tukey function

The most general form for the Tukey function is given by,

$$R(t) = \begin{cases} \frac{1}{2} \left[1 + \cos\left(\frac{\pi}{1-\alpha} \frac{2t}{t_m} + \frac{\pi}{1-\alpha} - \pi\right) \right], & \text{for } \frac{-t_m}{2} \leq t < \frac{-t_m}{2}\alpha \\ 1, & \text{for } \frac{-t_m}{2}\alpha \leq t \leq \frac{t_m}{2}\alpha \\ \frac{1}{2} \left[1 + \cos\left(\frac{\pi}{1-\alpha} \frac{2t}{t_m} - \frac{\pi}{1-\alpha} + \pi\right) \right], & \text{for } \frac{t_m}{2}\alpha < t \leq \frac{t_m}{2} \\ 0, & \text{otherwise,} \end{cases} \quad (\text{A1})$$

where α is called the tapering parameter [59, 60].

The Tukey function we have used in this communication is corresponding to $\alpha = 0$. In this case the above general expression takes the form,

$$R(t) = \begin{cases} \frac{1}{2} \left[1 + \cos\left(\frac{2\pi t}{t_m}\right) \right], & \text{for } |t| \leq \frac{t_m}{2} \\ 0, & \text{otherwise,} \end{cases} \quad (\text{A2})$$

which is corresponding to zero tapering. The Fourier transform of the above Tukey function (corresponding to zero tapering) is given by,

$$\tilde{R}(\omega) = \frac{1}{4\pi} \sin\left(\frac{\omega t_m}{2}\right) \left(\frac{2}{\omega} - \frac{1}{\omega + \frac{2\pi}{t_m}} - \frac{1}{\omega - \frac{2\pi}{t_m}} \right). \quad (\text{A3})$$

The full width at half maximum (FWHM) for the above function is given by $\Delta_{FWHM}^{(T)} = \frac{4\pi}{t_m}$, expressed in the units of energy, where the superscript T signifies the Tukey function [56]. To find the value of t_m the above expression for $\Delta_{FWHM}^{(T)}$ is equated to the value of the resolution width, 1.4 meV at FWHM, specified in the experimental observations corresponding to La_2CuO_4 .

The modified Tukey (MT) function we have used in our analysis is corresponding to 50% tapering, i.e. $\alpha = 0.5$, and is given by,

$$\mathcal{R}(t) = \begin{cases} \frac{1}{2}[1 - \cos(\frac{4\pi t}{t_m})], & \text{for } \frac{-t_m}{2} \leq t \leq \frac{-t_m}{4} \\ 1, & \text{for } \frac{-t_m}{4} \leq t \leq \frac{t_m}{4} \\ \frac{1}{2}[1 - \cos(\frac{4\pi t}{t_m})], & \text{for } \frac{t_m}{4} \leq t \leq \frac{t_m}{2} \\ 0, & \text{otherwise.} \end{cases} \quad (\text{A4})$$

Fourier transform of the above modified Tukey function is given by,

$$\tilde{\mathcal{R}}(\omega) = \frac{1}{4\pi} [\sin(\frac{\omega t_m}{2}) + \sin(\frac{\omega t_m}{4})] (\frac{2}{\omega} - \frac{1}{\omega + \frac{4\pi}{t_m}} - \frac{1}{\omega - \frac{4\pi}{t_m}}). \quad (\text{A5})$$

The full width at half maximum corresponding to the above function $\mathcal{R}(\omega)$ can be found out to be $\Delta_{FWHM}^{(MT)} \approx \frac{3.2\pi}{t_m}$, expressed in the units of energy. In this case, to find the value of t_m we have equated $\Delta_{FWHM}^{(MT)}$ to the value of the resolution width specified in the experiment.

- [1] H. Bethe, Z. Physik **71**, 205(1931).
- [2] Y. Endoh, et.al., Phys. Rev. Lett., **32**, 170(1974).
- [3] A. A. Katanin, V. Yu Irkhin, Physcis– Uspekhi, **50**(6), 613- 635(2007) *and references therein*.
- [4] J. Prokop et. al., Phys. Rev. Lett **102** 177206(2009).
- [5] M. Cwik et. al., Phys. Rev. Lett **102** 057201(2009).
- [6] F. Demmel and T. Chatterji, Phys. Rev. B **76** 212402(2007).
- [7] T. Chatterji et. al., Phys. Rev. B **76** 144406(2007).
- [8] F. Weber et. al., Phys. Rev. Lett **107** 207202(2011).
- [9] S. M. Yusuf et. al., Phys. Rev. B **84** 064407(2011).
- [10] H. Ulbrich et. al., Phys. Rev. B **84** 094453(2011).
- [11] H. J. Lewtas et. al., Phys. Rev. B **82** 184420(2010).
- [12] L. Braicovich et. al., Phys. Rev. B **81** 174533(2010).
- [13] Ranjan Chaudhury, *Spin dynamics of quantum spin models in layered systems– signature of Kosterlitz– Thouless scenario?* – presented at ULT 2011 (August 19– 22, 2011), held at KAIST, Daejeon, South Korea.

- [14] Yong-il Shin, *Creation of 2D Skyrmions in spin-1 polar Bose-Einstein Condensates* – presented at ULT 2011 (August 19–22, 2011), held at KAIST, Daejeon, South Korea.
- [15] S. W. Lovesey, *Theory of Neutron Scattering from Condensed Matter*(Oxford– Clarendon Press) 1986, Vol. 2, Chap: 8, 9.
- [16] I. U. Heilmann, et.al., Phys. Rev. B., **24**, 3939(1981).
- [17] J. K. Kjems and M. Steiner, Phys. Rev. Lett., **41**, 1137(1978).
- [18] M. Steiner, K. Kakurai, W. Knop, R. Pynn, J.K. Kjems, Solid State Comm., **41**, Pages 329-332 (1982).
- [19] L.V. Yakushevich, Journal of Biological Physics **24**, 131–139 (1999).
- [20] G. Reiter, Phys. Rev. Lett., **46**, 202(1981).
- [21] K. Hirakawa, H. Yoshizawa, K. Ubukoshi, J. Phys. Soc. Jpn., **51**, 2151(1982).
- [22] K. Hirakawa, et.al., J. Phys. Soc. Jpn. Part-2, **52**, 4220(1983).
- [23] M. T. Hutchings, J. Als-Nielsen, P. A. Lindgard and P. J. Walker, J. Phys. C: Solid State Phys., **14**, 5327-5345(1981).
- [24] M. T. Hutchings, P. Day, E. Janke and R. Pynn, J. Magn. Magn. Mater, **54-57**, 673(1986).
- [25] L. K. Alexander, N. Büttgen, R. Nath, A. V. Mahajan, and A. Loidl, Phys. Rev. B **76**, 064429 (2007).
- [26] D. G. Wiesler, et.al., Physica **136B**, 22-24(1986).
- [27] P. Steffens et.al., Phys. Rev. B., **83**, 054429(2011).
- [28] L. Capogna et. al.; Phys. Rev. B., **67**, 012504(2003).
- [29] G. Castilla, S. Chakravarty, and V. J. Emery, Phys. Rev. Lett. **75**, 1823 (1995).
- [30] Y. Endoh, et.al. Phys. Rev. B **37**, 7443 (1988).
- [31] K. Yamada et.al., Phys. Rev. B., **40**, 4557(1989).
- [32] L. Berger, Y. Labaye, M. Tamine, and J. M. D. Coey, Phys. Rev. B.,**77**, 104431, (2008).
- [33] A. Wachowiak, J. Wiebe, M. Bode, O. Pietzsch, M. Morgenstern and R. Wiesendanger, Science, **298**, 577 (2002).
- [34] R. P. Cowburn, D. K. Koltsov, A. O. Adeyeye, M. E. Welland, and D. M. Tricker, Phys. Rev. Lett, **83**, 1042, (1999).
- [35] B. Van Waeyenberge, Nature, **444**, 461 (2006).
- [36] H. Hauser, J. Hochreiter, G. Stangl, R. Chabicovsky, M. Janiba and K. Riedling,, J. Magn. Magn. Mater, **215**, 788 (2000).

- [37] J. McCord, J. Westwood, IEEE Trans. Magn., **37**, 1755, (2005).
- [38] J. M. Kosterlitz and D. J. Thouless: J. Phys. C **6** 1181(1973).
- [39] V. L. Berezinskii, Sov. Phys. JETP **32**, 493(1970); Sov. Phys. JETP **34**, 610(1972).
- [40] J. V. José, ed., 40 Years of Berezinskii–Kosterlitz–Thouless Theory, World Scientific (2013), Chap. 1.
- [41] D. L. Huber, Phys. Lett. **68A**, 125(1978); Phys. Rev. B. **26**, 3758(1982).
- [42] F. G Mertens, A. R. Bishop, G. M. Wysin and C. Kawabata, Phys. Rev. Lett, **59**, 117(1987); Phys. Rev. B. **39**, 591(1989).
- [43] M. E. Gouvêa, G. M. Wysin, A. R. Bishop, F. G. Mertens, Phys. Rev. B, **39**, 11840(1989).
- [44] A. R. Völkel, G. M. Wysin, A. R. Bishop and F. G. Mertens, Phys. Rev. B. **44**, 10066(1991).
- [45] G. M. Wysin and A. R. Bishop, Phys. Rev. B., **42**, 810 (1990).
- [46] P. W. Anderson, et.al, Princeton University Preprint, 1988.
- [47] R. Chaudhury, Indian J Phys, **66A**, 159 (1992)
- [48] S. Sarkar, S. K. Paul and R. Chaudhury, Eur. Phys. J. B, **85**, 380 (2012).
- [49] H. J. Mikeska, J. Phys. C: Solid St. Phys., **13**, 2913 (1980).
- [50] G. Shirane, S. M. Shapiro, and J. M. Tranquada, *Neutron Scattering with a Triple-Axis Spectrometer, Basic Techniques*, (Cambridge University Press) 2004, Chaps. : 1, 4.
- [51] F. Hippert, E. Geissler, Jean. L. Hodeau, E. L-Berna and Jean-R Regnard, *Neutron and X-Ray Spectroscopy, Grenoble Sciences*, Springer 2006, Chap: 11.
- [52] M. Takahashi, J. Phys. Soc. Jpn., **52**, 3592(1983).
- [53] R. C. Tolman, *The Principles of Statistical Mechanics*, (Dover Publication), 1976, Chap. XII
- .
- [54] M. T. Evans and C. G. Windsor, J. Phys. C., **6**, 495 (1973).
- [55] C. G. Windsor and J. Locke-Wheaton, J. Phys. C., **9**, 2749 (1973).
- [56] R. Chaudhury and B. S. Shastry, Phys. Rev. B. **37**, 5216(1988).
- [57] T. Thio, et.al, Phys. Rev. B., **38**, 905 (1988).
- [58] N. D. Mermin and H. Wagner, Phys. Rev. Letts. **17**, 1133 (1966); erratum: Phys. Rev. Letts. **17**, 1307 (1966).
- [59] F. J. Harris, Proceedings of The IEEE, **66**, 51(1978).
- [60] G. M. Jenkins and D. G. Watts, *Spectral Analysis and Its Applications*, (Holden-Day), 1968, Chap:6.

- [61] S. Sarkar, R. Chaudhury and S. K. Paul, arXiv:1410.5921v2 [**cond-mat.str-el**] (2015).
- [62] F. D. M. Haldane, Phys. Rev. Lett., **50**, 1153(1983).
- [63] E. Fradkin, M. Stone, Phys. Rev. B., **38**, 7215, (1988); E. Fradkin, *Field Theories of Condensed Matter Systems*, (Addison-Wesley, CA, 1991).
- [64] F. D. M. Halden, Phys. Rev. Lett, **61**, 1029(1988).
- [65] R. Chaudhury and S. K. Paul, Phys. Rev. B., **60**, 6234(1999).
- [66] R. Chaudhury and S. K. Paul, Mod. Phys. Lett. B, **16**, 251-259(2002).
- [67] R. Chaudhury and S. K. Paul, Eur. Phys. J. B, **76**, 391-398(2010).
- [68] Y. H. Chen, F. Wilczek, E. Witten and B. I. Helperin, Int. J. Mod. Phys. B, **3**, 1001 (1989).
- [69] C. M. Varma, arXiv:1502.00577 [cond-mat.str-el] (2015).